Section I: Basic and Applied Research

Thermodynamic Calculation of Phase Equilibria of the Bi-Sn-Zn System

Dmitri V. Malakhov, Xing Jun Liu, Ikuo Ohnuma, and Kiyohito Ishida

(Submitted 30 May 2000)

A thermodynamic assessment of the Bi-Sn-Zn ternary system was carried out by considering the experimental data including the phase equilibria and thermodynamic properties on the basis of the CALPHAD method. A set of optimized thermodynamic parameters has been obtained, which leads to a very good fit between calculation and experiments. In particular, the thermodynamic calculations in the Sn-rich portion are presented in view of the recent progress in Pb-free solder alloys.

1. Introduction

Numerous efforts have been undertaken in recent years to develop Pb-free substitutes for the lead-tin soldering alloys widely used in microelectronics. Systems containing Ag, Bi, Cu, In, Sb, Sn, Zn, and other elements have been the subjects of experimental investigation, but many of them remain unexplored. The methods of computational thermodynamics are known to be powerful tools to facilitate, accelerate, and simplify the search for proper Pb-free alloys. The Bi-Sn-Zn alloys are promising candidates for the development of Pb-free alloys. Although experimental investigations on phase equilibria of this system were carried out many years ago, thermodynamic assessment has not been carried out so far.

As a part of the thermodynamic database for microsolder alloys [1999Ohn, 2000Ohn], the purpose of the present work is to make a thermodynamic assessment of the Sn-Bi-Zn system on the basis of the experimental data by the CALPHAD method [1998Sau].

2. Survey of Previous Works

2.1 Thermodynamic Properties

Temperature and composition dependencies of the chemical potential of zinc in the liquid phase were investigated using mainly the electromotive force (EMF) technique [1959Ole, 1962Koz, 1966Pta, 1967Glu, 1968Lou, 1977Bal, 1985Mat], and magnitudes of errors were considered for optimization. Since $\Delta\mu_{Zn} = -2FE$, a random error can be given as $2F\Delta_{abs}E$. Sometimes the reported accuracy of voltage measurements is unrealistically high, and thus, it was decided to use max $(2F\Delta_{abs}E| \Delta\mu_{Zn}| \Delta_{rel}\mu)$ as a more realistic estimation of random error.

Dmitri V. Malakhov, Department of Materials Science and Engineering, McMaster University, Hamilton L8S 4M1, ON, Canada; and **Xing Jun Liu, Ikuo Ohnuma**, and **Kiyohito Ishida**, Department of Materials Science, Graduate School of Engineering, Tohoku University, Sendai 980-8579, Japan. Contact e-mail: ishida@material.tohoku.ac.jp.

Vapor pressures of zinc over Sn-Zn-Bi melts were measured by means of the Knudsen effusion method in the range of 317 to 387 °C [1961Yok]. The gas phase was assumed to contain only monomers, and the chemical potential $\mu_{Zn}^{L} = RT \ln (P_{Zn}/P_{Zn}^\circ)$ was evaluated with the dependence $P_{Zn}^0(T)$. The reported relative accuracy of pressure measurements is 3.24%; errors of temperature and composition were assumed to be 2 K and 0.001.

2.2 Phase Diagram

Experimental investigations of the Bi-Sn-Zn phase diagram date from the end of the nineteenth century when Wright and Thomson determined compositions of two coexisting liquids by chemical analysis of separated layers [1891Wri, 1892Wri]. The temperature ranges 600 to 700 °C and 700 to 800 °C were examined with averages of about 650 and 750 °C, respectively. Those results can be treated only as a semi-quantitative estimation because of the following: first, it has become firmly established that the upper critical temperature of liquid-liquid separation in the binary system Bi-Zn is located below 600 °C [2000Mal]; and second, the presence of tin increases the mutual solubility of bismuth and zinc. It follows that immiscibility cannot take place above 600 °C, but Wright and Thomsom observed a region of miscibility above 700 °C for melts with high Sn contents [1891Wri]. It is likely that the system was not allowed to reach equilibrium. For this reason, the data of Wright and Thomson were not utilized in the present optimization.

Muzaffar measured thermal arrests of 104 liquid alloys using cooling curves [1923Muz]. The first and second recorded arrests could be identified as reaching two- and three-phase equilibria, while the third corresponded to the eutectic transformation. Averaging of the latter values (91 points) gives $T = 129.87 \pm 0.15$ °C as the eutectic temperature. The experimental information gained was sufficient to delineate a projection of the liquidus surface, tie-lines of secondary separation, and a family of vertical sections. Since thermal arrests corresponding to liquid-liquid separation could not be observed under the experimental technique employed, the locations of the miscibility gap borders at different temperatures were not revealed. Muzaffar's data were used in the optimization, with $\Delta T = 2$ °C taken as the

random error of temperature recording. In addition to random errors, a significant bias error caused by supercooling phenomena can be suspected. In particular, the experimentally determined eutectic temperature is probably slightly lower than the equilibrium one. Nevertheless, since T_{eut} = 129.87 °C is a weak function of the initial liquid composition, it is considered to be a good estimation, one that should be reproduced with a high accuracy during optimization. This can be done if artificially enlarged statistical weights are employed.

The phase diagram by Jänecke [1937Jan] suggests 137 and 199 °C as the temperatures of eutectic transformations in the binary Bi-Sn and Sn-Zn systems, respectively. These values significantly differ from their modern counterparts 140.69 °C [1994Oht] and 192.5 °C [1999Oht]. The reliability of the reported ternary eutectic temperature 136 °C was questionable, and thus discarded from input data.

2.3 Thermodynamic Assessments

The first attempt to calculate the phase diagram of the system with computational thermodynamics was done by Oleari and Fiorani [1959Ole]. By using the EMF technique, they measured the chemical potential of zinc in the melt along constant ratios x_{Sn}/x_{Bi} = 1/9, 1/3, 1/1, and 3/1 in the temperature range 440 to 570 °C, and deduced analytical expressions for integral and partial properties of the liquid phase. They also computed miscibility gap boundries at 450, 500, and 550 °C and built a projection of the liquidus. One

can find several shortcomings in their model of the Bi-Sn-Zn system: first, homogeneous regions of terminal solid solutions were neglected; second, the calculated eutectic temperature 135 °C is more than five degrees higher than the directly measured value 129.87 °C [1923Muz]; and third, the eutectic composition of x_{Zn} = 0.03, x_{Bi} = 0.41, and x_{Sn} = 0.56 is located too close to the Bi-Sn side of the diagram. Actually the content of zinc in the liquid of eutectic composition exceeds 0.05.

Ptak and Moser treated their data on EMF measurements in terms of the Krupkowski model [1951Kru] and obtained analytical expressions describing the activities of components

Fig. 1 Distribution of weighted residuals for the different types of data

Table 1 Summary of the thermodynamic parameters in the Bi-Sn-Zn system used in the present assessment

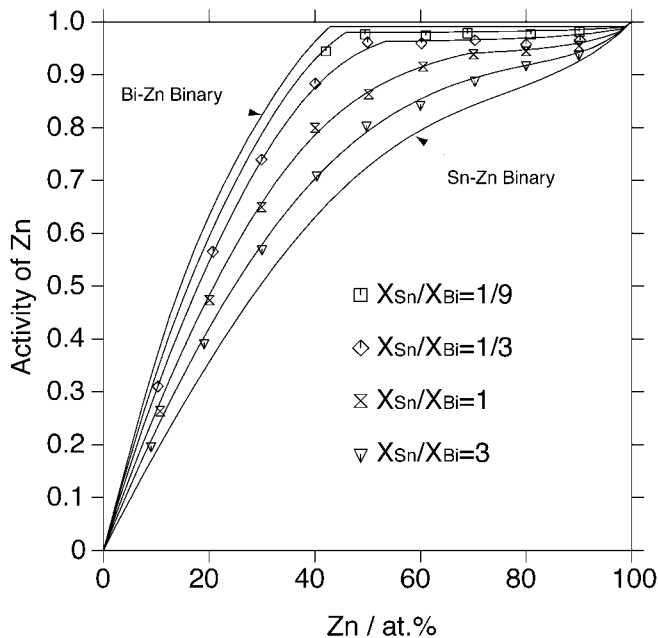| System	Parameters (J/mol)	Reference
Bi-Sn	$^0L_{BiSn}^L = 490.0 + 0.97*T$	[1994Oht]
	$^1L_{BiSn}^L = -30.0 - 0.235*T$	
	$^0L_{BiSn}^{bct} = 2120 - 1.44*T$	
	$^1L_{BiSn}^{bct} = -3710.0$	
	$^0L_{BiSn}^{rho} = 19720.0 - 22.6*T$	
	$^1L_{BiSn}^{rho} = -5760 + 11.834*T$	
Bi-Zn	$^0L_{BiZn}^L = 18,265.09 - 8.6763*T$	[2000Mal]
	$^1L_{BiZn}^L = -6061.21 + 0.79581*T$	
	$^2L_{BiZn}^L = -6422.6 + 11.72*T$	
	$^3L_{BiZn}^L = 7227.44 - 9.2905*T$	
	$^4L_{BiZn}^L = 21,123.07 - 27.147*T$	
	$^5L_{BiZn}^L = -20,747.56 + 22.0176*T$	
	$^6L_{BiZn}^L = -7600.36 + 13.16*T$	
	$^0L_{BiZn}^{hcp} = 35,000$	
	$^0L_{BiZn}^{rho} = 10,000$	
Sn-Zn	$^0L_{SnZn}^L = 12,710 - 9.162*T$	[1999Oht]
	$^1L_{SnZn}^L = -5360.0 + 3.45*T$	
	$^2L_{SnZn}^L = 835.0$	
	$^0L_{SnZn}^{bct} = 9260$	
	$^0L_{SnZn}^{hcp} = 40,000$	
Bi-Sn-Zn	$^0L_{BiSnZn}^L = -76,485.59 + 98.4963*T$	Present work
	$^1L_{BiSnZn}^L = 7048.7 - 9.25285*T$	
	$^2L_{BiSnZn}^L = -265.89 - 11.10087*T$	

Fig. 2 Calculated activity of Zn at 450 °C compared with the experimental data [1959Ole]
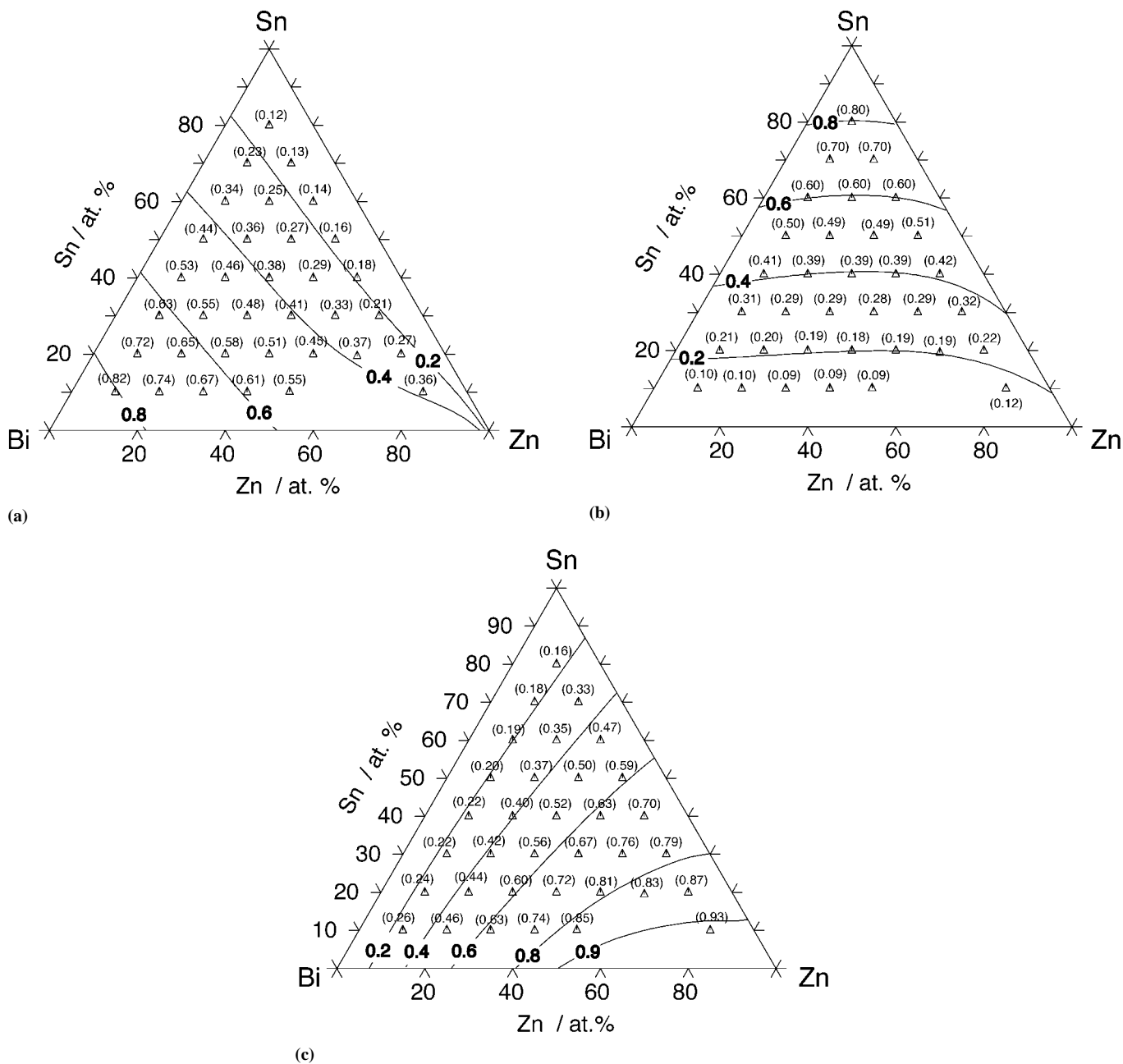
(a)

(b)

(c)

Fig. 3 Calculated activities of (**a**) Bi, (**b**) Sn, and (**c**) Zn at 551 °C compared with the experimental data [1966Pta]

in the liquid Bi-Sn-Zn melt [1966Pta]. The derived expressions were used to calculate ranges of limited solubility at $T = 440.85$, 483.85, 531.85, and 568.85 °C [1971Pta]. The extent of the miscibility gap in the binary Bi-Zn system reported in [1971Pta] is significantly wider than that found in the most recent optimization [2000Mal]. For example, the extent at $T = 568.85$ °C is from 67.5 to 95 at.% of Zn, while Malakhov gives 72 to 93% at the same temperature [2000Mal]. From the findings of Ptak and Moser [1966Pta, 1971Pta], the critical temperature of separation in the binary Bi-Zn melt exceeds 600 °C, although actually it is situated below 580 °C.

Bale *et al.* measured chemical potentials of zinc in the

quaternary Zn-Cd-Bi-Sn melt by the EMF method [1977Bal]. The results were used to construct a polynomial description of the excess Gibbs energy of the liquid phase. The polynomial expression was utilized by Pelton *et al.* to build a liquidus surface projection [1977Pel]; details of the calculations are given in [1980Lin]. As shown by Malakhov [2000Mal], the model of the liquid phase developed by Bale *et al.* has some dubious features. In particular, it leads to the top of the miscibility gap in the system Bi-Zn being located at the very high temperature 808.07 °C and it does not provide convexity of the liquid-liquid phase boundary. If the model does not work properly in one of the binaries, it can hardly be considered wholly satisfactory. If one recalls that the homogeneity
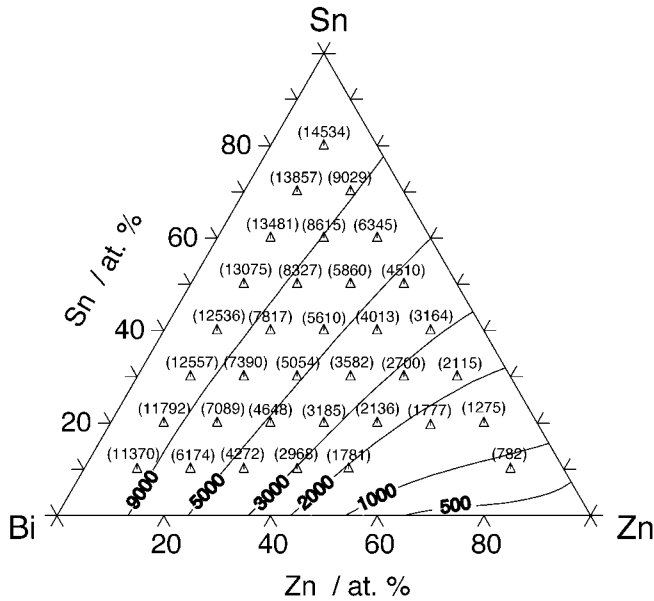
Fig. 4 Calculated chemical potential of Zn at 641 °C compared with the experimental data [1966Pta]

regions of the terminal solid solutions were neglected by Pelton *et al.* [1977Pel], it becomes clear that an exhaustive thermodynamic description of the system Bi-Sn-Zn had not been achieved.

3. Thermodynamic Model of the Gibbs Free Energy

Due to a lack of data on thermodynamic properties of terminal solid solutions as well as on their phase boundaries, only binary contributions were utilized, and the ternary terms were ignored.

In the case of the liquid phase, the availability of experimental data makes possible the inclusion in principle of a ternary term. Gibbs free energy of the liquid phase is described using the subregular solution model with the Redlich–Kister polynomials [1948Red], as follows:

$$G_m^L = \sum_{i=Bi,Sn,Zn} {}^0G_i^L x_i^L + RT \sum_{i=Bi,Sn,Zn} x_i^L \ln x_i^L$$
$$+ x_{Bi}^L x_{Sn}^L L_{Bi,Sn}^L + x_{Bi}^L x_{Zn}^L L_{Bi,Zn}^L$$
$$+ x_{Sn}^L x_{Zn}^L L_{Sn,Zn}^L + \Delta^{ex}G^{tern}$$

$$L_{i,j}^L = \sum_{m=0}^{n} {}^mL_{i,j}^L \cdot (x_i - x_j)^m$$

$$\Delta^{ex}G^{tern} = x_{Bi}^L x_{Sn}^L x_{Zn}^L (x_{Bi}^L \, {}^0L_{BiSnZn}^L + x_{Sn}^L \, {}^1L_{BiSnZn}^L$$
$$+ x_{Zn}^L \, {}^2L_{BiSnZn}^L)$$

where the coefficient ${}^mL_{i,j}^L$ is the parameters in the sub-binary system, and ${}^nL_{BiSnZn}^L$ may be temperature dependent and is optimized in our calculations.

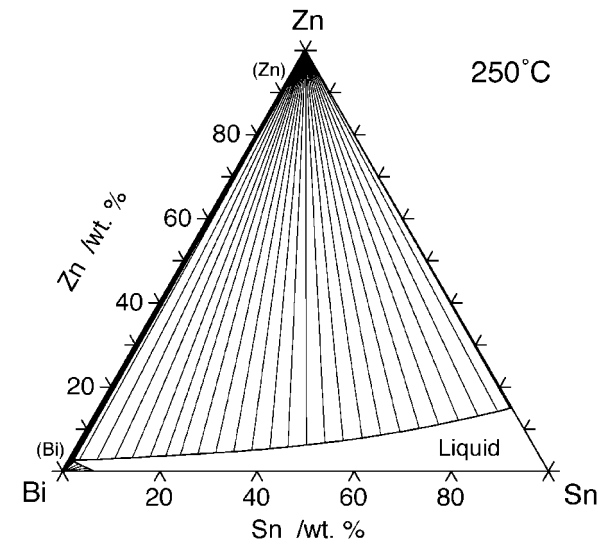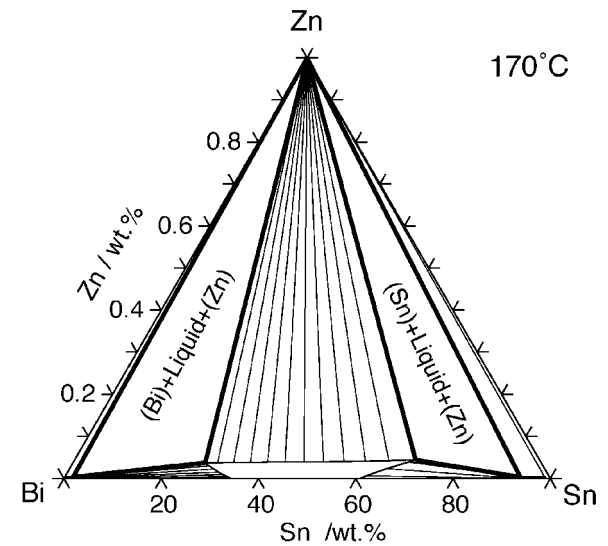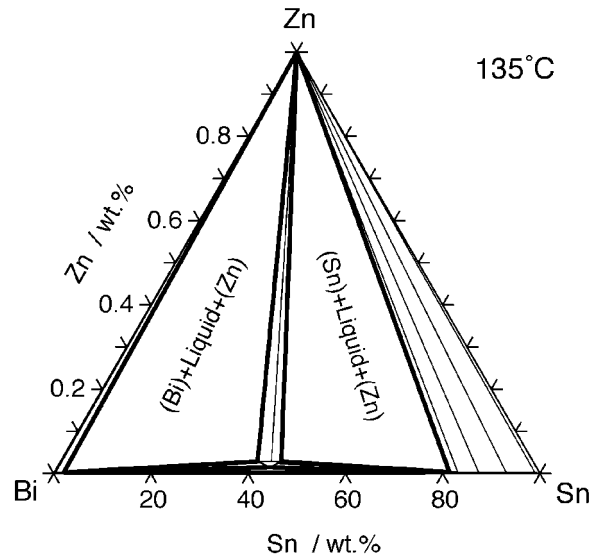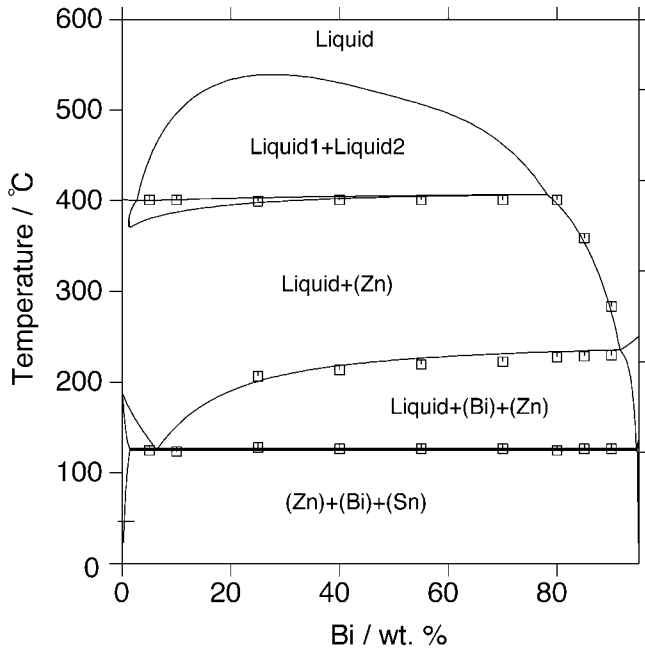All lattice stabilities were taken from [1991Din], except

Fig. 5 Calculated isothermal sections at 135, 170, and 250 °C

(a)
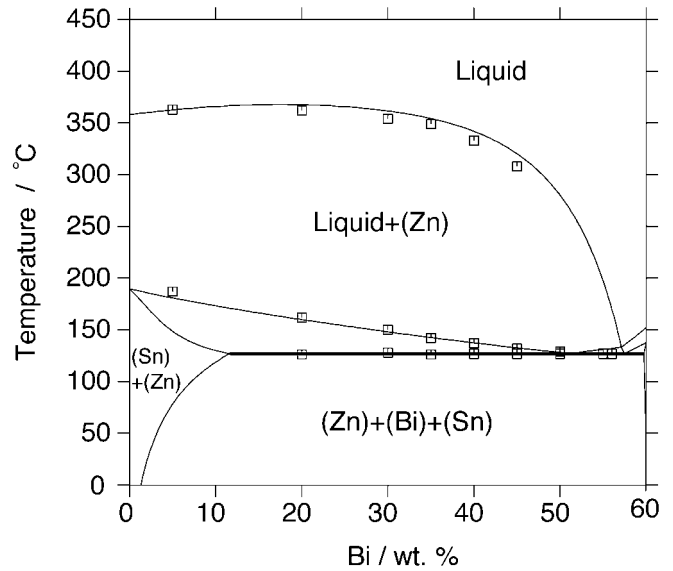
(b)

Fig. 6 Calculated vertical sections of (**a**) 5 wt.% Sn and (**b**) 40 wt.% Sn compared with the experimental data [1923Muz]
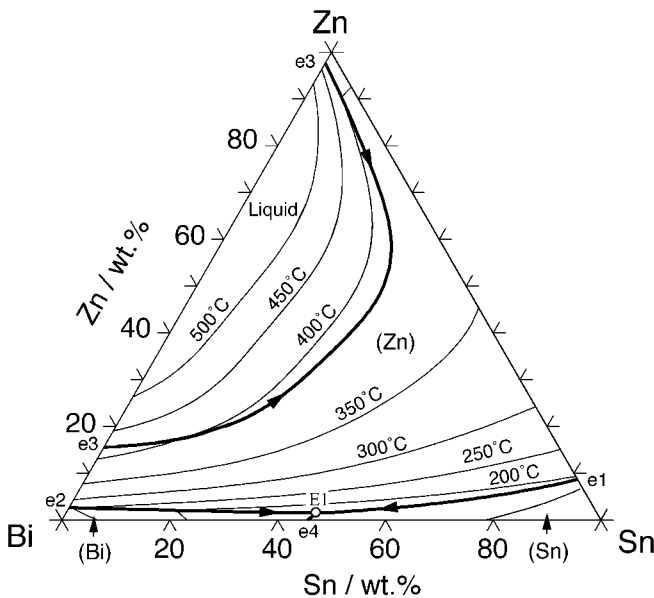

Fig. 7 Calculated projection of liquidus surface of the Bi-Sn-Zn system
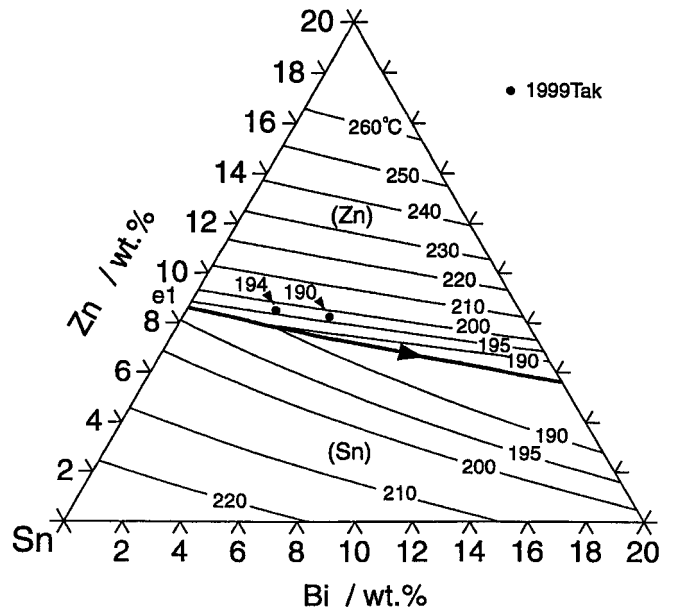

Fig. 8 Liquidus surface of the Sn-rich portion compared with the experimental data

$G_{Sn}^{hcp} - G_{Sn}^{bct} = 2400 - 3.1T$ [1988Kar], $G_{Zn}^{bct} - G_{Zn}^{hcp} = 10,000$ [1999Oht], and $G_{Zn}^{rhombo} - G_{Zn}^{hcp} = 2300 + 11.5T$ [1997Din]. A detailed explanation of how the latter function was evaluated can be found in [2000Mal].

The thermodynamic assessments of the Bi-Sn, Bi-Zn, and Sn-Zn binary systems were made by Ohtani and Ishida [1994Oht], Malakhov [2000Mal], and Ohtani *et al.* [1999Oht], respectively. The parameters of these binary systems were used in the present assessment.

4. Results

4.1 Optimization Results

Figure 1 demonstrates that weighted deviations corresponding to the partial Gibbs energy of Zn have reasonable values. The existence of a comparatively heavy negative tail corresponding to Muzaffar's data [1923Muz] can be

Table 2 Calculated characteristics of eutectic equilibrium

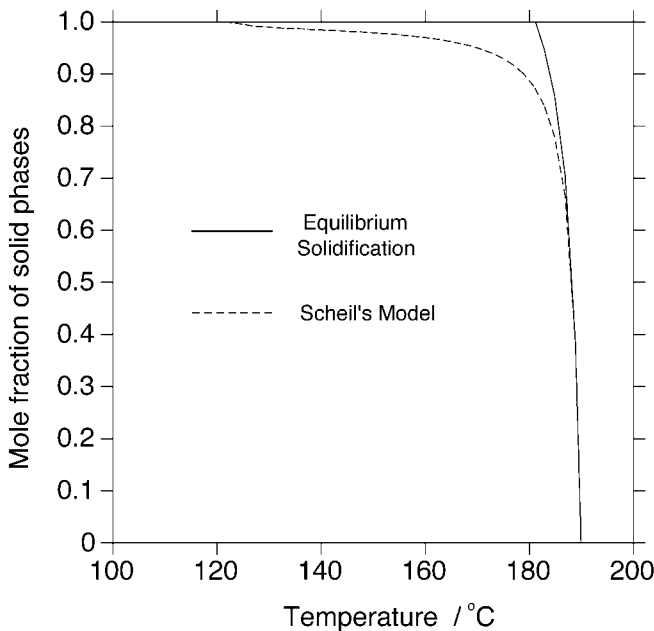| Reaction	Temperature (°C)	Phase	Composition at.% (wt.%)		
			Bi	Sn	Zn
L ↔ (Bi) + (Sn) + (Zn)	130	Liquid	39.39 (54.54)	54.35 (42.75)	6.25 (2.71)
		(Bi)	95.75 (97.75)	3.44 (1.99)	0.81 (0.26)
		(Sn)	14.03 (22.37)	85.41 (77.35)	0.56 (0.28)
		(Zn)	6.03×10^{-4}	4.23×10^{-4}	99.999
			(1.93×10^{-3})	$(7.68 \times 10{-4})$	(99.997)

Fig. 9 Phase fraction of solid *vs* temperature of the Sn-8 wt.% Zn-3 wt.% Bi alloy

explained if one remembers that supercooling might have taken place in his experiments where the cooling curve technique was employed.

The thermodynamic parameters of the liquid phase were optimized on the basis of the experimental data, and the values are given in Table 1. The covariance matrix is $s_{appr}^2 \times (t_\alpha(f))^2 \times (\mathbf{J}^T \mathbf{J})^{-1}$, where $s_{appr}^2 = \dfrac{1}{f} \sum_{i=1}^{m} \varepsilon_i^2 = 3.697684$ is the variance of approximation; $m = 1459$ is the number of measurements; ε_i is the weighted deviations; $n = 6$ is the number of coefficients; $f = m - n = 1453$ is the number of degrees of freedom; $\alpha = 0.975$ corresponds to the 95% two-sided probability; $t_\alpha(f)$ is a Student's critical point, and $\mathbf{J}$ is the Jacobian taken from the final iteration of TERGSS [1997Mal].

4.2 Calculation of Thermodynamic Properties and Phase Diagrams

According to the optimized parameters in the present assessment, all experimental data including the phase equilibria and thermodynamic properties can be reproduced very well. The calculated activity of Zn is compared with the

experimental data [1959Ole] in Fig. 2. Figures 3 and 4 show the thermodynamic data of the activity and chemical potential, respectively, where the agreement between calculated and observed values [1966Pta] is quite satisfactory. Figure 5 shows the calculated isothermal sections at 135, 170, and 250 °C. The characteristic features of the phase diagram in this ternary system are (1) the solubilities of Bi and Sn in (Zn) are negligibly small, (2) the solubility of Zn in (Bi) is also small, and (3) (Zn) directly equilibrates with liquid or (Bi) and (Sn). Figure 6 shows the phase equilibria of vertical sections at 5 wt.% Sn and 40 wt.% Sn, and it is seen that good agreement is obtained between the calculated results and experimental data [1923Muz]. The projection of the liquidus surface is presented in Fig. 7. In the Bi-Sn-Zn system, no experimental data for the isothermal sections and very limited information for the liquidus surface are available. Only a calculated liquidus surface in the entire composition range was presented by Pelton *et al.* [1977Pel], where the calculated eutectic reaction occurs at about 137 °C and 2.5 at.% Zn and 54 at.% Sn. In the present calculation, the eutectic reaction takes place at $T = 130$ °C with compositions of four equilibrium phases given in Table 2.

4.3 Phase Equilibria in the Sn-Rich Portion

Since the melting temperature of the eutectic Sn-Zn binary alloy is close to that of the Pb-Sn eutectic alloy, the Sn-Zn based Pb-free solders have been cited as very promising candidates [1994McC]. In view of this, the phase equilibria of the Sn-rich portion is practically important. Figure 8 shows the liquidus surface of the Sn-rich portion, recent experimental data [1999Tak] being included. Moreover, a Sn-8 wt.% Zn-3 wt.% Bi solder alloy has been developed and is being practically used for the packaging of personal computers [2000Suz]. The present assessment enables simulations of the solidification process [2000Ohn]. Two limiting cases of calculations were performed to predict the phase fractions as a function of temperature: one is equilibrium solidification based on the lever rule; and the other is based on the Scheil model, which assumes no back-diffusion in the solid phase and perfect mixing in the liquid phase. For most alloys, Scheil's calculation provides a prediction close to reality. Figure 9 shows the calculated phase fraction of solid *vs* temperature variation of Sn-8 wt.% Zn-3 wt.% Bi alloy under equilibrium and nonequilibrium solidification conditions. In comparison with the equilibrium solidification, the formation of the liquid phase due to segregation in Scheil's calculation increases the freezing range.

5. Conclusions

Thermodynamic assessment of the Bi-Sn-Zn ternary system has been carried out on the basis of the experimental data including phase equilibria and thermodynamic properties. The ternary parameter of the liquid phase was optimized, and good agreement was obtained between the calculated results and experimental data.

References

1891Ald: C.R. Alder-Wright and C. Thomsom: *Proc. R. Soc. London*, 1891, vol. 49, pp. 156-73.

1892Ald: C.R. Alder-Wright: *Proc. R. Soc. London*, 1892, vol. 50, pp. 372-95.

1923Muz: S.D. Muzaffar: *J. Chem. Soc.*, 1923, vol. 123, pp. 2341-54.

1937Jan: E. Janecke: *Z. Metallkd.*, 1937, vol. 29, pp. 367-73.

1948Red: O. Redlich and A.T. Kister: *Ind. Eng. Chem.*, 1948, vol. 24, pp. 345-48.

1951Kru: A. Krupkowski: *Bull. Acad. Pol. Sci. Lett.,* 1951, vol. 1, p. 15.

1959Ole: L. Oleari and M. Fiorani: *L. Ricerca Scientifica*, 1959, vol. 29, pp. 2219-29.

1961Yok: T. Yokokawa, A. Doi, and K. Niwa: *J. Am. Chem. Soc.*, 1961, vol. 65, pp. 202-05.

1962Koz: Z. Kozuka, J. Moriyama, and I. Kushima: *Denki Kagaku (J. Electrochem. Soc. Jpn.)*, 1962, vol. 30, pp. 591-96 (in Japanese).

1966Pta: W. Ptak and Z. Moser: *Archiwum Hutnictwa*, 1966, vol. 11, pp. 207-34 (in Polish).

1967Glu: J.V. Gluck and R.D. Pehlke: *Trans. TMS-AIME*, 1967, vol. 239, pp. 36-47.

1968Lou: R.L. Louvet, J.V. Gluck, and R.D. Pehlke: *Trans. TMS-AIME*, 1968, vol. 242, pp. 2369-71.

1971Pta: W. Ptak and Z. Moser: *Polonaise Sci. Bull. L'Acad. Ser. Techni.*, 1971, vol. 19, pp. 1-6.

1977Bal: C.W. Bale, A.D. Pelton, and M. Rigaud: *Z. Metallkd.*, 1977, vol. 68, pp. 69-74.

1977Luk: H.L. Lukas, E.T. Henig, and B. Zimmermann: *CALPHAD*, 1977, vol. 1, pp. 225-36.

1977Pel: A.D. Pelton, C.W. Bale, and M. Rigaud: *Z. Metallkd.*, 1977, vol. 68, pp. 135-40.

1980Lin: P.-L. Lin, A.D. Pelton, C.W. Bale, and W.T. Thompson: *CALPHAD*, 1980, vol. 4, pp. 47-60.

1985Mat: V.N.S. Mathur and M.L. Kapoor: *Z. Metallkd.*, 1985, vol. 76, pp. 16-23.

1988Kar: I. Karakaya and W.T. Thompson: *Bull. Alloy Phase Diagrams*, 1988, vol. 9, pp. 144-52.

1991Din: A.T. Dinsdale: *CALPHAD*, 1991, vol. 15, pp. 317-425.

1994McC: M. McCormack and S. Jin: *J. Electr. Mater.*, 1994, vol. 23, pp. 687-90.

1994Oht: H. Ohtani and K. Ishida: *J. Electr. Mater.*, 1994, vol. 23, pp. 747-55.

1995Oht: H. Ohtani, K. Okuda, and K. Ishida: *J. Phase Equil.*, 1995, vol. 16, pp. 416-29.

1997Din: A.T. Dinsdale: National Physical Laboratory, Teddington, Middleses, UK, private communication, 1997.

1997Mal: D.V. Malakhov: *CALPHAD*, 1997, vol. 21, pp. 391-400.

1998Sau: N. Saunders and A.P. Miodownik: *CALPHAD*, Pergamon, Lausanne, 1998.

1999Oht: H. Ohtani, M. Miyashita, and K. Ishida: *J. Jpn. Inst. Met.*, 1999, vol. 63, pp. 685-94.

1999Ohn: I. Ohnuma, X.J. Liu, H. Ohtani, and K. Ishida: *J. Electr. Mater.*, 1999, vol. 28, pp. 1164-71.

1999Tak: T. Takemoto, M. Takahashi, R. Ninomiya, Y. Nakahara, H. Tai, and A. Matsunawa: *5th Symp. on Microjoining and Assembly Technology in Electronics*, Mate '99, Yokohama, Japan Welding Society, Tokyo, 1999, pp. 325-30.

2000Mal: D.V. Malakhov: *CALPHAD*, 2000, vol. 24, pp. 1-14.

2000Ohn: I. Ohnuma, X.J. Liu, H. Ohtani, and K. Ishida: in *Functional Materials*, K. Grassie *et al.*, eds., WILEY-VCH Verlag Gmbh, Weinheim, 2000, pp. 69-74.

2000Suz: M. Suzuki, H. Matsuoka, E. Kono, H. Sakai, M. Igarashi, and K. Onodera: *6th Symp. on Microjoining and Assembly Technology in Electronics*, Mate '2000, Yokohama, 2000, pp. 325-28.